UNITECR 2025

Sustainability Meets Intelligence

SHAPING THE FUTURE OF REFRACTORIES

BOOK OF PROCEEDINGS

UNITECR CANCUN 2025

ANODES BASED ON MgO-C RECYCLATES AND 316L STEEL FOR PROSPECTIVE ALUMINIUM FUSED-SALT ELECTROLYSIS APPLICATION

Patrick Gehre[1], Serhii Yaroshevskyi[1], Patricia Kaiser[1], Nora Brachhold[1], Jana Hubálková[1], Christos G. Aneziris[1]
[1]TU Bergakademie Freiberg, Institute of Ceramics, Refractories and Composite Materials, Freiberg, Germany

ABSTRACT

Every year, approx. 28 million tons of used refractories accumulate worldwide. The majority of them are used as aggregates for road construction (downcycling) or are deposited in landfills. For ecological and economic reasons, an increased research potential was identified in recent years, dedicated to increasing the recycling rate and finding new markets and application fields with a higher value of the refractory recyclates. The study presents the current findings of the development of inert electrodes for the aluminum fused-salt electrolysis composed of steel and MgO gained from MgO-C recyclates. To withstand the chemical attack of molten aluminum and cryolitic melts, the metal-ceramic composites were preoxidized (PO) at 800 °C, 900 °C, and 1000 °C. The microstructure after each PO thermal treatment was analyzed. After PO at 800 °C, a $(Cr,Fe)_3O_4$ spinel-like phase and Fe-O Mg-O solid solution form. After PO at 900 °C, a larger amount of the Fe-O Mg-O solid solution and a $(Cr,Fe)_2O_3$ solid solution around the steel grains was identified. Furthermore, the electrical conductivity of the metal-ceramic-composites preoxidized at 900 °C amounts to $1.49 \cdot 10^2$ S·cm^{-1} and hence is in the range of carbon, which exhibits a value of $1.54 \cdot 10^2$ S·cm^{-1}. Additionally, the impact of different preoxidation treatments at 900 °C by applying furnaces equipped with electrical heating, natural gas burner, and microwave plasma burner on the microstructure was investigated.

INTRODUCTION

Aluminum (Al) is extensively utilized in various areas of modern engineering and manufacturing due to the combination of low density with high machinability, high mechanical strength, corrosion resistance, and recyclability[1]. To produce Al, bauxite ore is refined to alumina (Al_2O_3) and then subjected to the Hall-Héroult process[2]. This process involves the dissolution of Al_2O_3 in molten cryolite (Na_3AlF_6) followed by the electrolysis of the melt. Today, the most commonly used setup for the Hall-Héroult cell is a carbon lining that forms the cathode paired with consumable graphite anodes. When a direct current passes through the cell, aluminum ions (Al^{3+}) are reduced at the cathode, forming molten aluminum at the bottom of the cell, while oxygen ions (O^{2-}) are oxidized at the graphite anode, producing carbon dioxide (CO_2). Today, producing 1 ton of primary aluminum indirectly generates ~8.9 tons of CO_2 for necessary electricity production and 1.5 tons of CO_2 directly during electrolysis with consumable graphite electrodes[3]. In recent years, increasing attention has been directed toward the development of ceramic, cermet, and metallic inert anodes (e.g. $NiFe_2O_4$, copper-nickel alloys, and various metal-ceramic composite materials[4]) for the Hall-Héroult process. The application of such anodes not only reduces CO_2 emissions but also enhances the efficiency of the process in terms of material usage. Despite different matrix materials, all of them obtain the same common feature: a protective oxide layer, which is either preformed during production or formed during the operation of the anode, helps to withstand cryolite attack during electrolysis[5]. The most important characteristics of a material for inert anodes are high chemical stability and resistance to oxidation combined with sufficient electrical conductivity[6]. A material that could meet these requirements is a composite based on steel and MgO. MgO–C refractory bricks naturally contain a wide range of metallurgical residues after serving in the vessels such as basic oxygen furnace (BOF) and steel ladle. However, up to 70–75 % of the material still consists of valuable MgO grains.

Therefore, this research explores the possibility of utilizing such recycled material to produce steel–ceramic composite materials that might be used to manufacture inert anodes for aluminum electrolysis cells. This research focuses on manufacturing and both investigates and compares phases that form during preoxidation of the metal-ceramic anodes at 800 °C, 900 °C, and 1000 °C and after applying different heating technologies.

MATERIALS AND METHODS

Materials

To produce the steel-ceramic composite material, AISI 316L stainless steel powder (TLS Technik, Germany) was used as the matrix material. Tab. I lists its chemical composition. The true density is 7.62 g·cm^{-3} and the particle size (d_{90}) is <51 µm.

Tab. I: Chemical composition (wt.%) of 316L stainless steel powder (next to Fe).

Cr	*Ni*	*Mn*	*Mo*	*Si*	*C*	*Al*
16.85	10.47	0.89	2.09	0.40	0.020	0.065

MgO-C recyclates (Refratechnik Steel, Germany) of reprocessed MgO–C bricks were provided with a particle size of 0 to 1 mm. The carbon content of the recycled MgO–C fraction is ~19 wt.%. First, the 0–1 mm MgO-C fraction was sieved to get a <125 µm powder. The true density of the sieved MgO-C powder is 3.58 g·cm^{-3} and the particle size (d_{90}) is <109 µm. Afterwards, the MgO-C powder underwent a carbon burn-out procedure at 1000 °C for 24 h to receive MgO with a chemical composition given in Tab. II.

Tab. II: Chemical composition (wt.%) of MgO powder (<125 µm) after carbon burn-out process.

MgO	*Al_2O_3*	*K_2O*	*CaO*	*Fe_2O_3*	*Na_2O*	*Rest*
93.03	1.31	0.12	1.59	0.78	0.68	2.045

Preparation of aggregates

Due to the significant difference in thermal expansion coefficients between steel and MgO, composite granules were manufactured using additives[7]. The volumetric ratio MgO to steel of the mixture was 40:60 vol.-%. As a result, mixing these coarse granules with fine-grained raw powder allows the pressing of compounds with large dimensions without cracking. Only granules < 3.2 mm in diameter were used. The debinding of the granules was performed min with a heating rate of 2 K·min^{-1} to 200 °C, 0.5 K·min^{-1} to 500 °C, and a cooling rate of 0.5 K·min^{-1}. The sintering was conducted at 1350 °C for 2 h under an argon atmosphere (99.999 %) with a heating rate of 5 K·min^{-1} to 1350 °C and a cooling rate of 5 K·min^{-1} to 300 °C. Such pre-sintered granules will not experience any thermal-related shrinkage during subsequent sintering procedures.

Manufacturing of electrodes

The coarse-grained composite material consists of 70 vol.% of the sintered granules and 30 vol.% of a mixture of fine MgO and steel powder with the same volumetric ratio (40:60). This material mixture was cold isostatically pressed (CIP EPSI 300-250 x 1000 Y, Temse, Belgium) in a latex mold with a diameter of 35 mm and a height of 80 mm at 150 MPa. The pressed samples were debinded and sintered with the same parameters that were used for the

granules. After sintering, the cylinder was cut into disc-shaped specimens with a thickness of 8 mm (Fig. 1). A set of four discs was selected for the EBSD/SEM analysis: as-sintered state ("AS specimen") and 3 specimens in preoxidized states. Preoxidation thermal treatment was carried out at 800 °C ("PO800"), 900 °C ("PO900"), and 1000 °C ("PO1000") for 24 h in air.

To investigate the impact of the sintering technology on the surface condition, preoxidation at 900 °C for 4 h was performed in an electrically heated (E), microwave-plasma burner-heated (MWP), and gas-burner-heated (G) furnace.

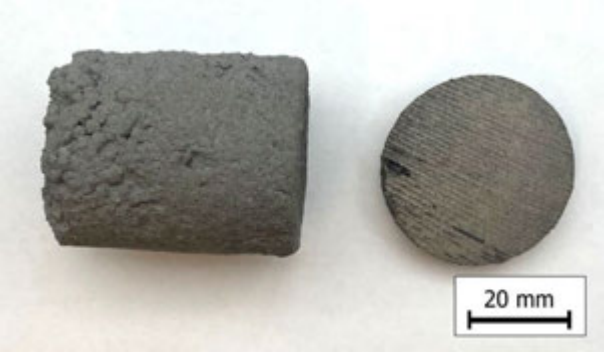

Fig. 1: CIP pressed coarse-grained steel-ceramic composite cylinder after sintering and cut disc specimen in the as-sintered state.

Microscopically analyses

Microstructural analysis was conducted using SEM-FIB Amber (Tescan, Czech Republic). Additionally, EBSD (Bruker Nano, Germany) was used for point analysis of the crystalline structures of the specimens. Each specimen was analyzed in a region directly at the surface. Phases were identified with the help of the inorganic crystal structure database (ICSD, FIZ Karlsruhe, Germany). Since EBSD is a local analysis providing information exclusively about a relatively small area, each sample was scanned twice with the investigated area shifted by 1 mm sideward. Additionally, the surface of the specimens after preoxidation using different heating technologies was examined using laser scanning microscopy (VK-X 1000, Keyence, Germany).

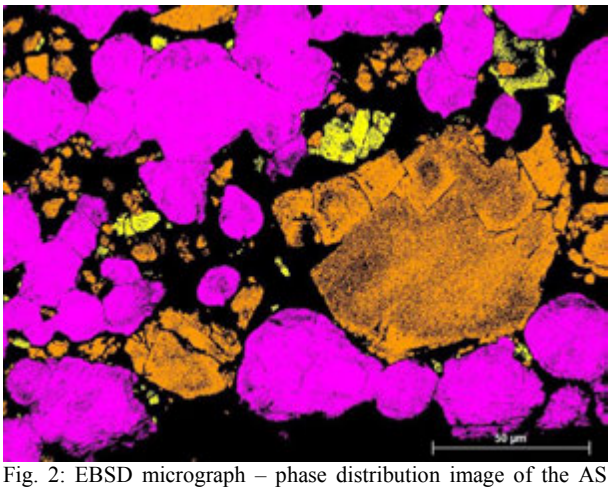

Fig. 2: EBSD micrograph – phase distribution image of the AS specimen: orange: MgO; pink: steel; yellow: monticellite (Ca– Mg–O phase).

RESULTS AND DISCUSSION

As-sintered specimen

The result of the EDX/EBSD analysis of sample AS is displayed in Fig. 2. The phases are displayed with separate colors, with black denoting either non-crystalline phases or pores of the material. The image represents MgO grains (orange) and steel grains (pink, cubic phase). No sign of steel oxidation was observed. Additionally, a calcium-magnesium silicate phase was detected as a secondary phase. EBSD point analyses identified that phase as monticellite, which is a well-known impurity of MgO raw materials and hence originates from spent and oxidized MgO-C recyclates used as raw material for the production of the electrodes.

Specimen after preoxidation at 800 °C

Compared to the as-sintered sample (AS), significant changes in the materials' phase compositions were observed in the PO800 specimen (Fig. 3). Reactions occurred at the edge and between the steel and MgO particles, but the MgO (orange) and steel grains (pink) as well as monticellite (yellow) exhibit still an internal structure almost identical to the respective grains of the non-oxidized specimen. At the grain boundaries of the steel grains, an area with a higher concentration of Cr, Mo, and Ni compared to the core of the steel grain could be identified. In addition, reactions are visible at the grain boundaries of the MgO grains where new Mg–Fe–oxide phases (blue) have been gradually formed. Due to the cubic nature of their crystalline structure and the varying content of Mg and Fe, it is presumed that it might be a halite-like Mg–O Fe–O solid solution. Similar phases were detected by XRD in fine-grained metal-ceramic composites based on MgO and 316L stainless steel[8]. The halite-like solid solution explains the variability of the Fe–Mg ratio within the blue Mg–Fe oxide phase, as the ratio between Fe–O and Mg–O compounds gradually changes depending on the distance to MgO and steel grains. In the following, this phase will be referred to Mg–O Fe–O solid solution halite-like phase.

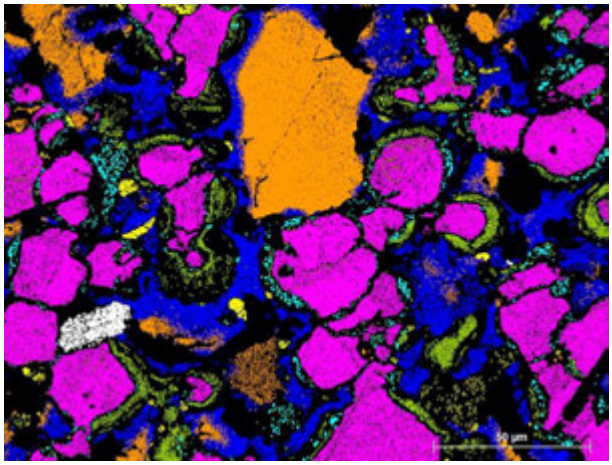

Fig. 3: EBSD micrograph – phase distribution image of the PO800 specimen: orange: MgO; pink: steel; yellow: monticellite; blue: Mg–O Fe–O solid solution halite-like phase; turquoise: $(Cr,Fe)_2O_3$; green: $(Cr,Fe)_3O_4$ spinel; white: Mg-Al–spinel.

The steel grains are surrounded by Fe-containing Cr–O phases (turquoise) with trigonal structure as well as cubic oxide phases (green). The Fe-containing Cr–O phase is most likely a $(Cr,Fe)_2O_3$ solid solution with a corundum-like structure. Trigonal crystals are typical of such corundum structures, and a solid solution explains variability in chemical composition. Therefore, both phases could not be indexed. The main difference between these two phases is the crystal structure. The cubic phase may be represented by $(Fe,Cr)_3O_4$ solid solution, which forms a cubic spinel-like structure. The trigonal corundum Fe,Cr oxide phase (turquoise) can only be detected at the sides of the steel grains not being in contact with the MgO grains. In contrast, the cubic spinel-like phase (green) formed between the steel grain (pink) and the Mg–O Fe–O solid solution halite-like phase (blue) resulting in a gradient transition from the steel grain, over the $(Fe,Cr)_3O_4$ spinel, the Mg–O Fe–O solid solution halite-like phase, to the MgO grain (orange). Furthermore, during the formation of such a gradient, due to the loss of iron from

the steel grain at its grain boundaries, there is an area formed that exhibits a higher Cr–Ni–Mo concentration compared to the initial steel composition.

Additionally, Mg-Al spinel (white) was detected in the sample. The Mg-Al spinel structure shows a high concentration of Al and hence originates from the MgO recyclate powder that has been contaminated by Al during the operation in the steel plant.

Specimen after preoxidation at 900 °C

Compared to the sample after preoxidation at 800 °C, the oxidation reactions were considerably more pronounced in the PO900 specimen resulting in a higher amount of the Mg–O Fe–O halite-like phase with a clearly observable gradient reaction between Fe oxides and MgO grain (Fig. 4).

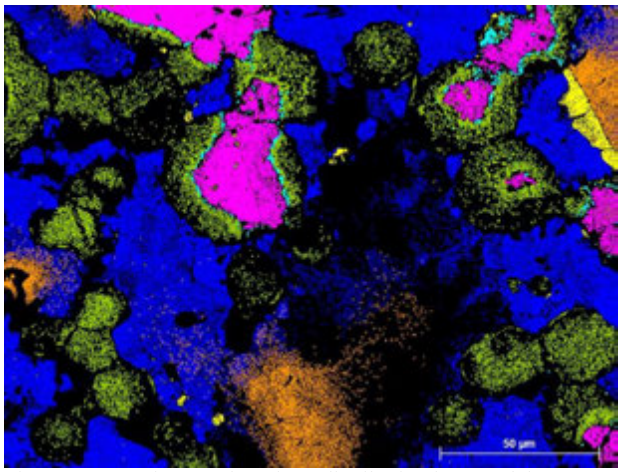

Fig. 4: EBSD micrograph – phase distribution image of the PO900 specimen; orange: MgO; pink: steel; yellow: monticellite; blue: halite-like Mg–O Fe–O solid solution; turquoise: $(Cr,Fe)_2O_3$ corundum; green: $(Cr,Fe)_3O_4$ spinel.

The area around the steel grains contains a high amount of Cr with considerably lower amounts of Fe and Ni as displayed in Fig. 5. This can be explained by reaction of Cr with Fe and their oxidation, which forms a thin layer of $(Cr,Fe)_2O_3$ corundum phase at the grain boundaries of the steel grains (turquoise) gradually transforming into $(Cr,Fe)_3O_4$ spinel-like phase (green) with increasing distance to the steel grain (pink). The oxidation of Cr and Fe is followed by the diffusion of Fe into the halite-like Fe–O MgO solid solution, whereas Cr does not tend to react with MgO (orange). It is also remarkable that Ni either remained inside the steel grain or with accompanied Fe in the spinel-like Fe–Cr–O phase. Additionally, hematite Fe_2O_3 was detected in the microstructure.

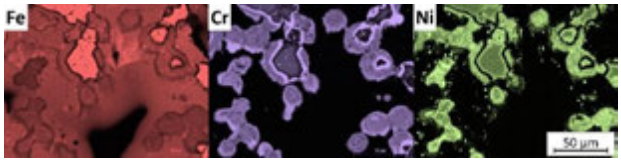

Fig. 5: EDX element distribution in the PO900 specimen.

Specimen after preoxidation at 1000 °C

The microstructure of the center of the PO1000 specimen is very similar to that of the PO900 specimen and is dominated by steel grains that are surrounded by a gradient transition from Fe–Cr–O corundum phase into a Fe–Cr–O spinel phase (Fig. 6). However, an important difference is the presence of Cr-rich metallic planar phases inside the steel grains. Overall, the PO1000 specimen shows a higher degree of oxidation compared to the sample PO900.

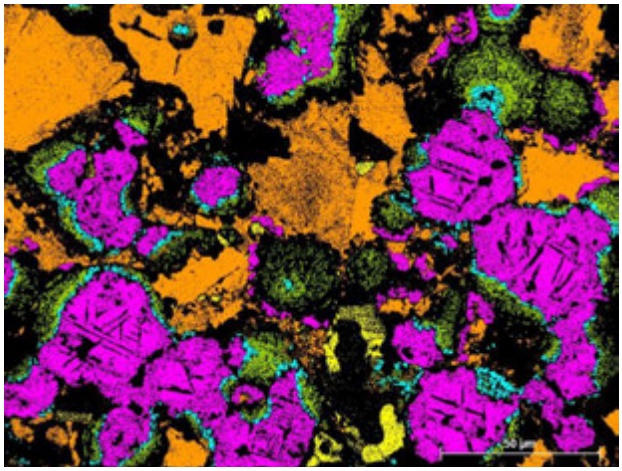

Fig. 6: EBSD micrograph – phase distribution image of the PO1000 specimen: orange: MgO; pink: steel; yellow: monticellite; turquoise: $(Cr,Fe)_2O_3$ corundum; green: $(Cr,Fe)_3O_4$ spinel.

After the PO at 1000 °C, all analyzed MgO grains at the surface of the sample showed a reaction with Fe oxides resulting in the formation of the halite-like Fe–O Mg–O solid solution (Fig. 7). Even though no steel grains can be observed in the microstructure, the outer layer is rich in the $(Cr,Fe)_3O_4$ spinel phase (green), Fe_2O_3 (red), and a Fe-Mg-O spinel phase (olive). The differences in the chemical composition of the $(Cr,Fe)_3O_4$ spinel and the Fe-Mg-O spinel phase at the outside of the sample have been confirmed by EBDS analysis. Compared to the $(Cr,Fe)_3O_4$ spinel phase, the Fe-Mg-O spinel phase shows a noticeably higher amount of Fe and is present at the bottom of the investigated area. In the periphery of the hematite grains, no alloying elements could be detected. Hence, a higher temperature leads to more pronounced oxidation of Fe that can be found in the surface layers of the composite material.

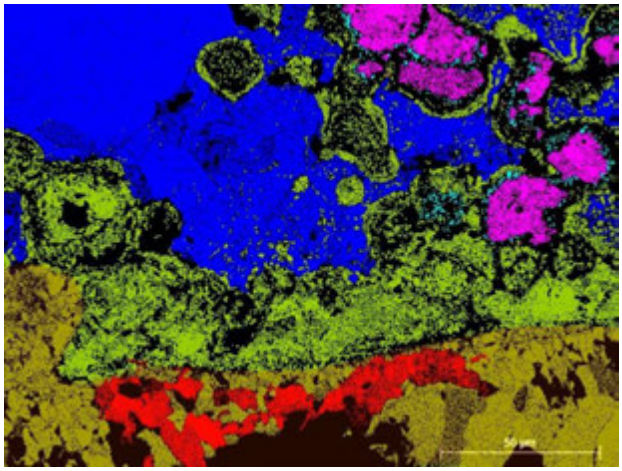

Fig. 7: EBSD micrograph – phase distribution image of the PO1000 specimen: pink: steel; blue: halite-like Mg–O Fe–O solid solution; turquoise: $(Cr,Fe)_2O_3$ corundum; green: $(Cr,Fe)_3O_4$ spinel; red: Fe_2O_3 hematite; olive: Fe-Mg-O spinel phase.

Considering the preoxidation in an electrical furnace, it can be stated that a temperature of 800 °C is too low to provide a proper amount of oxide phases at the surface serving as a protective layer against corrosion by molten aluminum and cryolite. Even though after preoxidation at 900 °C the specimen shows exposed MgO grains at the surface, which is unfavorable for the corrosion resistance in contact with cryolite, all steel grains are covered with a protective solid solution of Fe–O Mg–O and spinel phases. During preoxidation at 1000 °C, the sample underwent extensive oxidation

and is fully covered with thick oxide layers, including Fe–Mg-O spinel phase and Cr-rich spinel phase at outer boundaries.

Previous studies of metal–ceramic composite material based on MgO–316L 40–60 composition proved an electrical conductivity after preoxidation at 900 °C of approx. 150 $S \cdot cm^{-1}$ at room temperature[7]. A conductivity level above 200 $S \cdot cm^{-1}$ is considered as an excellent conductivity. Even if the PO1000 specimen is fully covered by a Fe–Mg spinel layer acting as a protection against corrosion, its electrical conductivity is below the sensitivity range of the measurement setup and therefore is considered not to have sufficient electrical conductivity. Hence, a preoxidation at 900 °C of the coarse-grained composite material based on MgO recyclates and steel 316L is the best compromise to fulfil the corrosion resistance as well as the electrical conductivity requirements.

Investigation of the technology of preoxidation

To investigate the impact of different peroxidation treatments on the surface condition, sintered uniaxial pressed samples prepared from fine-grained powder were preoxidized at 900 °C for 4 h in an electrically heated, microwave-plasmaburner-heated, and gas burner-heated furnace. Fig. 8 confirms that a preoxidation at 900 °C considerably changes the surface morphology of the MgO-steel composites compared to the as-sintered state, even after 4 h processing time. On the one hand, the surface shows significant discoloring. While the surface after thermal treatment in an electrically heated and gas burner-heated furnace shows no difference in color compared to the as-sintered state, a preoxidation with the aid of a microwave-plasma burner (MWPB) results in a change in color from light-grey in the as-sintered state to a mixture of light-grey and brass. Oppelt et al. noticed a discoloring of sintered disk-shaped MgO specimens manufactured from MgO raw materials that differ in their Fe_2O_3 content and that were treated by a microwave-plasmaburner at 1300 °C[9]. Based on the study of Melko et al. reporting that NO_x potentially reacts with iron species altering their oxidation state[10], these changes of the iron ions might be responsible for the change in color.

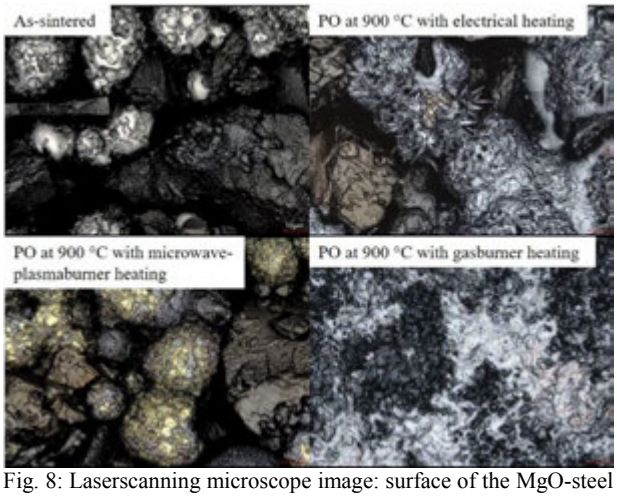

Fig. 8: Laserscanning microscope image: surface of the MgO-steel composite materials in the as-sintered state as well as after preoxidation at 900 °C for 4 h in an electrically heated, microwave-plasmaburner-heated, and gas burner-heated furnace.

On the other hand, the preoxidation process results in different surface macrostructure. The spherical steel particles connected to a continuous MgO matrix dominate the as-sintered surface. Some of the particles are interconnected with each other. Besides the mentioned change in color, a preoxidation with an MWPB does not significantly change the macrostructure, but the steel particles show more interconnections after PO at 900 °C for 4 h with MWPB. After PO in an electrically heated furnace, the steel can hardly be distinguished from the matrix as it shows a high degree of interphases among themselves and hence form another nearly continuous structure next to the MgO. At higher magnification, needle-like structures are visible growing at the surface of some granules. In contrast, a preoxidation with gas burners results in a macrostructure with a very different character consisting of a mixture of white/light grey and dark-grey areas that are interfused with each other. The steel particles are no longer visible and the surface appears more homogeneous compared to the other PO states.

CONCLUDING REMARKS

Metal-ceramic composites based on 316L steel and recycled MgO-C were successfully manufactured using cold isostatic pressing and pre-sintered agglomerates to introduce coarse grains into the composite material. The ceramic phase included MgO–C recyclates and sintering was conducted at 1350 °C under Ar atmosphere. Preoxidation thermal treatments at 800 °C, 900 °C, and 1000 °C were performed to study phase formation and oxidation behavior. During oxidation treatment, Fe migration from steel grains toward MgO leads first to the $(Cr,Fe)_2O_3$ phase followed by $(Cr,Fe)_3O_4$ spinel-like phase formation. In proximity to MgO grains, an Mg–O Fe–O solid solution phase was detected. With Fe tending to oxidize, the solid solution with MgO followed by Cr-rich phases is formed. The $(Cr,Fe)_3O_4$ phase is predominantly present at lower temperatures, while Mg–O Fe–O structures tend to be formed at higher temperatures, which indicates that more atoms of Fe migrate toward MgO grains. After preoxidation at 1000 °C, the formation of a Fe–Mg–O spinel phase was detected. All MgO grains reacted with steel forming a solid solution with FeO as well as a Fe–Mg–O spinel. After all MgO was consumed by this reaction, excessive Fe is oxidized to the hematite phase.

ACKNOWLEDGEMENTS

The authors gratefully acknowledge the financial support of the German Research Foundation (DFG) for funding the research as part of the Research Training Group GRK 2802 (project number 461482547).

REFERENCES

[1]Haynes WM, Lide DR, Bruno TJ. CRC Handbook of Chemistry and Physics. 97th ed. Boca Raton: CRC Press: 2016.
[2]Kermeli P, Weer PH, Crijns-Graus W et al. Energy efficiency improvement and GHG abatement in the global production of primary aluminium. Energy Effic. 2014; 8:629-66.
[3]Vassiliadou V, Peppas A, Taxiarchou M. A mathematical and software tool to estimate the cell voltage distribution and energy consumption in aluminium electrolysis cells. Mater Proc. 2021; 116(5):1-14.
[4]Galasiu I, Galasiu R, Nicolescu C. Metallic inert anodes for aluminium electrolysis. 1st ed. Hoboken: John Wiley & Sons; 2010.
[5]Haggerty JS, Sadoway DR. Investigation of materials for inert electrodes in aluminum electrodeposition cells. DOE report DOE/ID/12380-18. 1987.
[6]Gibilaro M, Meyer P, Massot L et al. Influence of operating conditions on cermet inert anode corrosion in cryolite for aluminium production. Corros Sci. 2021;192:109773.
[7]Yaroshevskyi S, Weigelt C, Malczyk P et al. Steel ceramic composite anodes based on recycled MgO–C lining bricks for applications in cryolite/aluminum melts. Open Ceram. 2023;16:100458.
[8]Malczyk P, Zienert T, Kerber F et al. Corrosion-resistant steel–MgO composites as refractory materials for molten aluminum alloys. Materials 2020;13:4737.
[9]Oppelt M, Dietze C, Dudczig S et al. Thermal treatment of MgO refractories in a pilot furnace heated with microwave plasma burner. J Eur Ceram Soc. 2025;45:117146.
[10]Melko JJ, Ard SG, Fournier JA et al. Exploring the reactions of Fe^+ and FeO^+ with NO and NO_2. J Phys Chem. 2012;116:11500-8.